https://www.scirp.org/journal/jbise
J. Biomedical Science and Engineering,
2024, Vol. 17, (No. 4), pp: 83-95

Simulation and Experimental Study of Staple Line Reinforcementin Surgery

Chengjie Hu[1], Jian Zhang[2]

[1]School of Health Science and Engineering, University of Shanghai for Science and Technology, Shanghai, China;
[2]Department of Colorectal Surgery, The Second Affiliated Hospital of Naval Medical University, Shanghai, China

Correspondence to: Jian Zhang, txzhangjian@126.com
Keywords: Staple Line Reinforcement, Surgical Anastomosis, Soft Tissue Damage, Finite Element Analysis, Leak-Proof Performance Experiments
Received: February 3, 2024 **Accepted:** March 31, 2024 **Published:** April 3, 2024

ABSTRACT

The aim of this study was to evaluate the effectiveness of BM (basement membrane) and SIS (small intestine submucosa) composite extracellular matrix staple line reinforcement in surgical procedures through finite element modelling simulations and leak-proof performance experiments. The mechanical analyses of soft tissues with and without staple line reinforcement were performed by establishing finite element models of three tissues, namely, stomach, intestine and lungs, under the use scenarios of different anastomosis staple models; and the leak-proof performance of the staple line reinforcement was evaluated by simulating leak-proof experiments of gastric incision margins, intestinal sections, and lung incision margins *in vitro*. The results showed that the equivalent average stresses of the staple line reinforcement were increased by 20 kPa - 68 kPa in gastric and intestinal tissues, and 8 kPa - 22 kPa in lung tissues. and that the BM and SIS composite extracellular matrix staple line reinforcement could strengthen the anastomotic structure, and at the same time disperse the high stresses of the anastomosed tissues, which could effectively reduce the postoperative complications such as anastomotic bleeding and anastomotic leakage, and provide a safer and more effective optimized design for surgical mechanical anastomosis. It can effectively reduce postoperative complications such as anastomotic bleeding and anastomotic leakage, and provide a safer and more effective optimized design for surgical mechanical anastomosis.

1. INTRODUCTION

In surgery, staplers are used to connect or reconstruct broken body tissues, which has the advantages

of easy operation, short operation time and fast postoperative recovery compared with traditional manual suturing. However, it is often used clinically for various reasons that still cannot completely avoid the occurrence of postoperative complications such as anastomotic leakage, anastomotic bleeding and infection. In the U.S. medical device adverse event reports from 1992 to 2016, a total of 75,415 failures and 676 deaths were anastomosis-related surgeries, with 92.4% of the deaths resulting from intraoperative tissue damage and 17.2% of the postoperative deaths related to tissue infection [1]. Anastomotic leaks also have an impact on postoperative overall survival, occurring in 5.1% of 1722 patients who underwent radical colorectal cancer resection, and their 5-year overall survival rate was 44.3%, compared with 64% who did not experience anastomotic leaks [2].

The stress distribution exerted on soft tissues by anastomotic staple forming has a direct impact on the quality of anastomotic suturing procedures [3]. Appropriate stress distribution ensures the stability of the anastomotic site and prevents over-anastomosis leading to tissue ischemia and inflammation, or insufficient stress leading to tissue hemorrhage and anastomotic leakage [4]. Currently, some antioxidant nanomedicines can control tissue ischemia and inflammation when considered during surgery [5], an absorbable staple line reinforcement on the anvil and staple compartment surfaces of the anastomosis can effectively reduce the stress concentration around the anastomotic staple, provide uniform dispersion of stress, effectively reduce the occurrence of anastomotic hemorrhage and anastomotic leakage [6], and promote tissue healing and tissue remodeling. Commonly used staple line reinforcement sheet materials include polyglycolic (PGA), expanded polytetrafluoroethylene (ePTFE), bovine pericardium (BP), porcine small intestine submucosa (SIS), etc. The synthetic polymer polyglycolic acid is a material with good biodegradability, and it was found in clinical trials that the use of polyglycolic acid reinforcement sheets (Neoveil™, Gunze Ltd., Japan) may cause in vivo inflammation and postoperative tissue adhesions due to high degradation rates [7]; polytetrafluoroethylene reinforcement sheets (Seamguard®, W. L. Gore and Associates, United States) has good biological inertness and biocompatibility, but may cause foreign body reactions due to its non-degradability [8]; the biomaterial bovine pericardial reinforcement sheet (Peri-Strips Dry®—PSD) has been shown to reduce extra cavitaryhemorrhage [9], and its collagenous fibers and elastic structure can provide tissue vascular regeneration and cellular infiltration; Downey [10] concluded that while bovine pericardial material reinforcement sheets can withstand better intraluminal pressures compared to SIS reinforcement sheets, this material is non-absorbable and can cause other rare complications. The use of reinforcement patches made of absorbable porcine small intestinal submucosal material (SIS, Surgisis®; Cook, Inc., Bloomington, IN) in the staple line prevents mechanical anastomotic leakage and has better biocompatibility [11]. Wong [12] tested a novel buttress made from the same synthetic absorbable materials used in VICRYL & PDS sutures brands (polyglactin 910 & polydioxanone), key characteristics examined included strength, absorption, security on the anvil and cartridge during tissue manipulation, abrasion, hemostasis and tissue healing. Cheng [13] [14] and others experimentally found that the use of BM (basement membrane) and SIS composite extracellular matrix reinforcement patches possessed superior tissue repair and regenerative efficacy, and significantly reduced the incidence of adverse reactions in the repair area, making them an ideal material for bio-anastomotic staple line reinforcement patches.

In order to investigate the effect of using BM/SIS composite matrix reinforcement sheet on soft tissue damage as well as anastomotic pressure during anastomotic nail forming, this paper takes three anastomotic models of stomach, intestines and lungs as an example, and establishes a model by finite element method to study the force of anastomotic nail anastomotic tissues in the anastomotic nail without reinforcement sheet and with reinforcement. And the leak-proof performance test of stomach, intestine and lung with staple line reinforcement is also carried out to provide reference for the optimal design of surgical mechanical anastomosis.

2. FINITE ELEMENT MODELLING SIMULATION OF SOFT TISSUE ANASTOMOSIS

2.1. Mechanical Model of Soft Tissue Anastomosis

Soft tissue anastomosis is achieved by pressing the tissue through the closure between the anvil and

the staple compartment of the staple to a staple-forming height and shape suitable for the staple. By pressing the handle and pushing the staple within the staple holder of the staple compartment, the soft tissue is first stapled through so that the staple reaches the offset seat under force and bends into a B-shape to staple the soft tissue together [15]. The blade within the staplers then cuts the soft tissue to form a closed staple line.

Without considering the interaction between the soft tissues, the force model of the staple and the soft tissues during the interaction is similar to that of a needle piercing the soft tissues [16] and can be expressed as Equation (1):

$$f_{staple}(x) = f_{stiffness}(x) + f_{cutting}(x) + f_{friction}(x) + f_{tissue}(x) + f_{anvil}(x) + f_{afriction}(x) \quad (1)$$

where: x is the displacement of the tip portion of the staple, $f_{staple}(x)$ is the penetration force of the staple, $f_{stiffness}(x)$ is the dorsal membrane resistance, $f_{cutting}(x)$ is the cutting force, $f_{friction}(x)$ is the friction between the staple and the soft tissue, $f_{tissue}(x)$ is the pressure of the soft tissue on the staple, $f_{anvil}(x)$ is the force of the anvil of the staple on the staple, $f_{afriction}(x)$ is the friction between the anvil of the anvil of the anvil of the staple and the staple.

The mechanical model of the anastomotic staple and soft tissue after the anastomotic tissue is completed is shown in **Figure 1(a)**, and the mechanical model of the anastomotic staple line reinforcement (SLR) loaded is shown in **Figure 1(b)**. The force of the anastomotic staple piercing the soft tissue is much smaller than the force between the anastomotic staple and the anvil, and the pierced anastomotic staple can be considered as a rigid body compared to the soft tissue.

2.2. Geometric Modelling

The staple is generally made of a biologically sound titanium alloy as the material, and in this paper, the staple of Echelon FlexTM GST system (Johnson & Johnson, Inc., USA) with a diameter of about 0.22 mm was used for the study. The relevant parameters of different colored staples and the corresponding thickness of the anastomotic tissue are shown in **Table 1**.

Six different soft tissue models were established, three models of stomach, intestine and lung without loading the staple line reinforcement and three models of stomach, intestine and lung with loading the staple line reinforcement. The thickness δ of the gastric, intestinal and lungs tissue models to be anastomosed was set to 3.3 mm, 2.6 mm and 2.0 mm, respectively [17-19]. The tissue force of each tissue model was calculated under the compression of different sizes of anastomotic staples, and a total of eighteen groups of anastomotic tissue models were established, as shown in **Table 2**. The models were built with SolidWorks 2022 and imported into ABAQUS 2022 for finite element analysis. As shown in **Figure 2**, the thickness of the staple line reinforcement was measured using a CHY-CA model thickness gauge produced by Jinan Saicheng Electronic Technology Co. The measurement points included three positions at the top, bottom and middle of the reinforcement piece. The average of these measurements was considered as the thickness of the sample., which was 0.10 mm, and the model length, width, and height dimensions were 15 mm × 15 mm × 0.10 mm. The soft tissues were simplified into a single-layer material structure [20], and the geometric model dimensions were 15 mm × 10 mm × δ, and the constructed model is shown in **Figure 3**.

2.3. Material Properties and Mesh Division

The staple is made of titanium, which has a modulus of elasticity of 96,000 MPa and a Poisson's ratio of 0.36 [21]. The staple is bent during the forming process, and the effect of heat exchange on the staple formation will be disregarded due to the short time period and the little heat exchange between the staple and the surrounding medium. In this paper, the tissue models are all regarded as incompressible isotropic hyperplastic materials, and the widely applicable Ogden hyperplastic constitutive relation is used, with the strain potential energy expression as Equation (2).

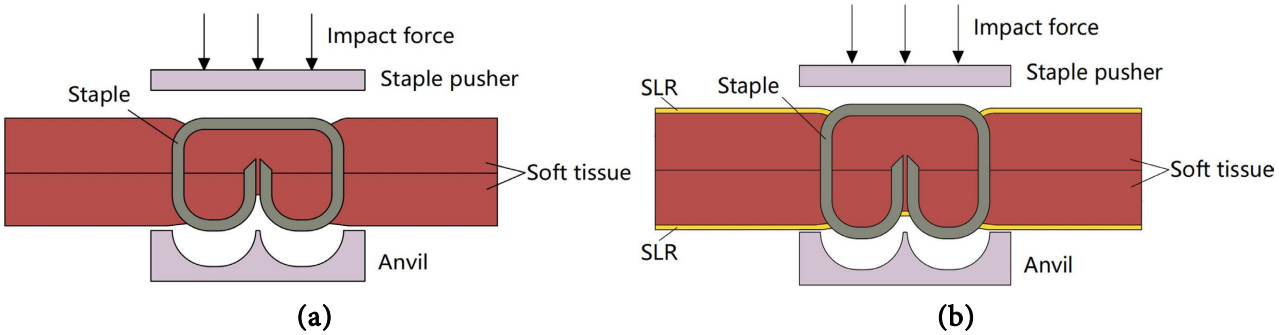

Figure 1. (a) Mechanical model of the staple forming process without reinforcement; (b) Mechanical model of the staple forming process with reinforcement.

Table 1. Relevant parameters of staple and corresponding anastomotic tissue thickness.

Staple cartridge	Open staple height (mm)	Closed staple height (mm)	Tissue thickness (mm)
White	2.6	1.0	1.0 - 2.0
Blue	3.6	1.5	1.5 - 2.4
Gold	3.8	1.8	1.8 - 3.0
Green	4.1	2.0	2.0 - 3.3
Black	4.2	2.3	2.3 - 4.0

Table 2. Tissue model and corresponding stapler specifications.

Tissuetype	Staple cartridge	Reinforcement	Group numbering
Stomach	Black	N	1
	Black	Y	2
	Green	N	3
	Green	Y	4
	Gold	N	5
	Gold	Y	6
Intestine	Green	N	7
	Green	Y	8
	Gold	N	9
	Gold	Y	10
	Blue	N	11
	Blue	Y	12
Lungs	Gold	N	13
	Gold	Y	14
	Blue	N	15
	Blue	Y	16
	White	N	17
	White	Y	18

Y stand for have staple line reinforcement, N for not have staple line reinforcement.

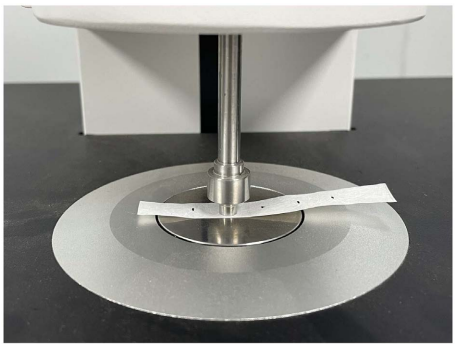

Figure 2. Using a thickness gauge to test the sample, take the average of the thickness of the top, bottom and middle of the sample as the thickness of the sample.

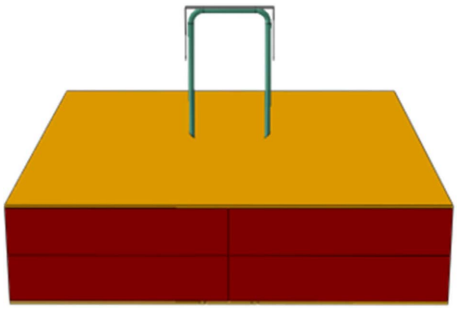

Figure 3. The model of the tissue with staple line reinforcement.

$$W = \sum_{i=1}^{N} \frac{\mu_i}{\alpha_i^2} \left(\lambda_1^{\alpha_i} + \lambda_2^{\alpha_i} + \lambda_3^{\alpha_i} - 3 \right) \tag{2}$$

where: λ denotes the principal strain elongation; μ and α are material constants. According to the literature [22-24], the fitting coefficients μ = 3.001 kPa, α = 11.56 for the stomach, μ = 3.281 kPa, α = 7.939 for the intestine, and μ = 0.453 kPa, α = 9.5 for the lungs, and the properties of the material damage were set according to the way of the unit-damage failure [25], and the material parameters of the staple reinforcement line were provided by Zhuoruan Medical Technologies (Suzhou) Co., Ltd. (China). Eight-node hexahedral cell meshing of soft tissues was performed with cell type C3D8R, which has higher accuracy compared to tetrahedral and is used to simulate the hyper elasticity intrinsic model with good results. At the same time, in order to improve the accuracy, encryption was carried out in the contact part of the staple, The total number of grid nodes for the lung tissue as shown in **Figure 4** is 35,287 and the number of cells is 29,400, the mesh division has an eccentricity of 5. Hexahedral meshing is also used for the staple line reinforcement and the staple, which is not repeated here because the object of this paper is a tissue model.

2.4. Contact Algorithm, Constraints and Loads

In order to allow the body of the staple to be fully embedded in the tissue, the contact between the staple body and the tissue, and the contact between the staple body and the reinforcement were all surface-junction contacts, and the penalty function contact algorithm was chosen for the contact analysis, and the contact friction coefficient between the soft tissue and the staple was set to 0.1. The binding constraints were set between the soft tissue and the reinforcement. The tissue model was punctured along the

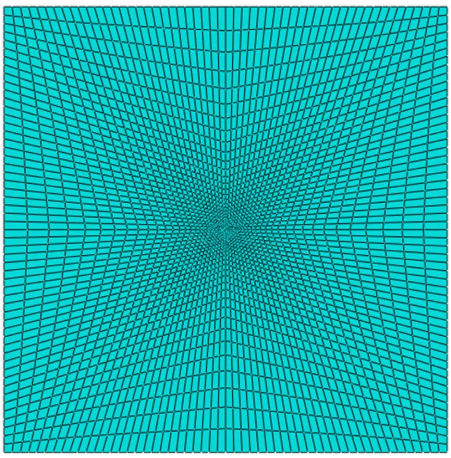

Figure 4. Model meshing.

direction normal to the contact point, and fixation was set around the soft tissue, as well as limiting all displacements of the staple except in the direction of indentation.

3. LEAK-PROOF PERFORMANCE OF THE STAPLE LINE REINFORCEMENT

In order to better evaluate the leak-proof performance of the staple line reinforcement for the anastomosis, three groups of leak-proof performance experiments were designed for different tissues. They are simulated gastric incision margin leakage test, simulated intestinal section leakage test and simulated lung incision margin leakage test.

The equipment and materials used for the experiments included an Echelon luminal linear cutting staple line and staple cartridge, a micro air pump, a pressure gauge, a three-way silicone tube, a water bath, and a staple line reinforcement. The injection port of the tissue being tested was ligated to one end of a three-way silicone tube, the other end was connected to a pressure gauge, and the third end of the silicone tube was connected to a miniature air pump. The flow rate of the air pump should not be too high in order to prevent the error of the test due to the high rate of change of air pressure, and the flow rate of the micro air pump was set at 1.2 L/min. The group that used the staple line reinforcement for the anastomosis was set as the experimental group, and the group that used the stapler for the direct anastomosis was set as the control group.

3.1. Simulated Stomach Cutting Edge Leakage Test

Five intact fresh pig stomachs of domestic pigs were prepared for the experimental group and the control group respectively, and the stomachs of each group were cut and anastomosed at the same part, trying to make the test status of the two groups as consistent as possible. As shown in **Figure 5(a)**, install the experimental device and check the airtightness of the whole set. Observe the stomach leakage and record the pressure value when the stomach leaks.

3.2. Simulated Intestinal Section Leakage Test

Five fresh small intestinal tissues of domestic pigs were obtained from the abattoir, washed of intestinal excreta and checked for intactness of the intestinal wall. From each pig small intestine adjacent to each other, two 12 cm sections of small intestine tissue were cut and divided into experimental and control groups, trying to make the thickness as well as the mechanical properties of the small intestines of each test group consistent. As shown in **Figure 5(b)**, the anastomosed small intestines were placed in water, the leakage of the intestinal section was observed, and the pressure value at the moment of intestinal leakage was recorded.

(a) (b) (c)

Figure 5. (a) Simulated gastric incision margin leakage test. (b) Simulated intestinal section leakage test. (c) Simulated lung cutting edge air leakage test.

3.3. Simulated Lung Cutting Edge Leakage Test

Five intact fresh pig lungs of domestic pigs were prepared for the experimental and control groups respectively, and similar parts were found on each lung tissue, and the lung tissues were wedged closed respectively, so that the anastomosis shapes of the experimental and control groups were the same. As shown in. (a) Simulated gastric incision margin leakage test. (b) Simulated intestinal section leakage test., the anastomosed lung tissue was placed in a water tank, and the air leakage from the cut edge of the lung in water was observed, and the pressure value of the lung leakage was recorded.

4. RESULTS AND ANALYSES

4.1. Stress Distribution of Tissue Anastomosis

The Von Mises equivalent stress distribution after tissue anastomosis as shown in shows that: in the same tissue model, the stress in the anastomotic part shows an increasing trend with the decrease of the staple formation height; in the case of the same staple formation height, the stress in its anastomotic part increases with the thickness of anastomotic tissue. In the gastric tissue model (a), the average value of the stresses applied to the tissue models (Group 1, Group 3, Group 5) not loaded with the staple line reinforcement was in the range of 100 kPa, and the average stresses applied to the tissue models (Group 2, Group 4, Group 6) loaded with the staple line reinforcement were increased in the range of 20 kPa - 68 kPa. Due to the similarity in the mechanical properties of the gastric and intestinal tissues, the stresses applied to the intestinal tissues with the staple line reinforcement line were increased by 20 kPa - 68 kPa in the intestinal tissue model (b). The intestinal tissues subjected to the mouth reinforcement piece showed similar changes in the stresses. The lung tissue model (c) has a thickness of 2.0 mm, and the mean values of the stresses applied to the tissues loaded with staple line reinforcement were increased by 8 kPa to 22 kPa compared to the tissues not loaded with staple line reinforcement, and the thin tissues did not have as much stress increase as the thick tissues. This means that the change in stress in the gastric and intestinal tissues after loading the reinforcement is greater than the change in the intestinal tissues. The difference in stresses on the anastomosing surface gradually increased for the three tissues after loading the staple line reinforcement. Since the size of the tissue modelled was larger than the actual anastomosis portion of the model, and the edge portion of the tissue model was not pressed by the staple, does not directly reflect whether the anastomotic stress distribution was more even or not (**Figure 6**).

Stress cloud comparisons were performed using thin and thick tissues as examples. For the anastomosis of lung tissue of 2 mm thickness, in the case of blue staple, the tissue model without reinforcement is shown in **Figure 7(a)**, the stress in the blue area of the tissue edge in contact with the staple is obviously insufficient, with a minimum of 900 Pa. The tissue model with reinforcement is shown in **Figure 7(b)**, the stress in the anastomotic portion is significantly increased and more evenly distributed. For the anastomosis of 3.2 mm thickness in the gastric tissue in the case of black staple, **Figure 7(c)** shows the concentration of stress in the region where the tissue is in contact with the staple without the use of the reinforcement.

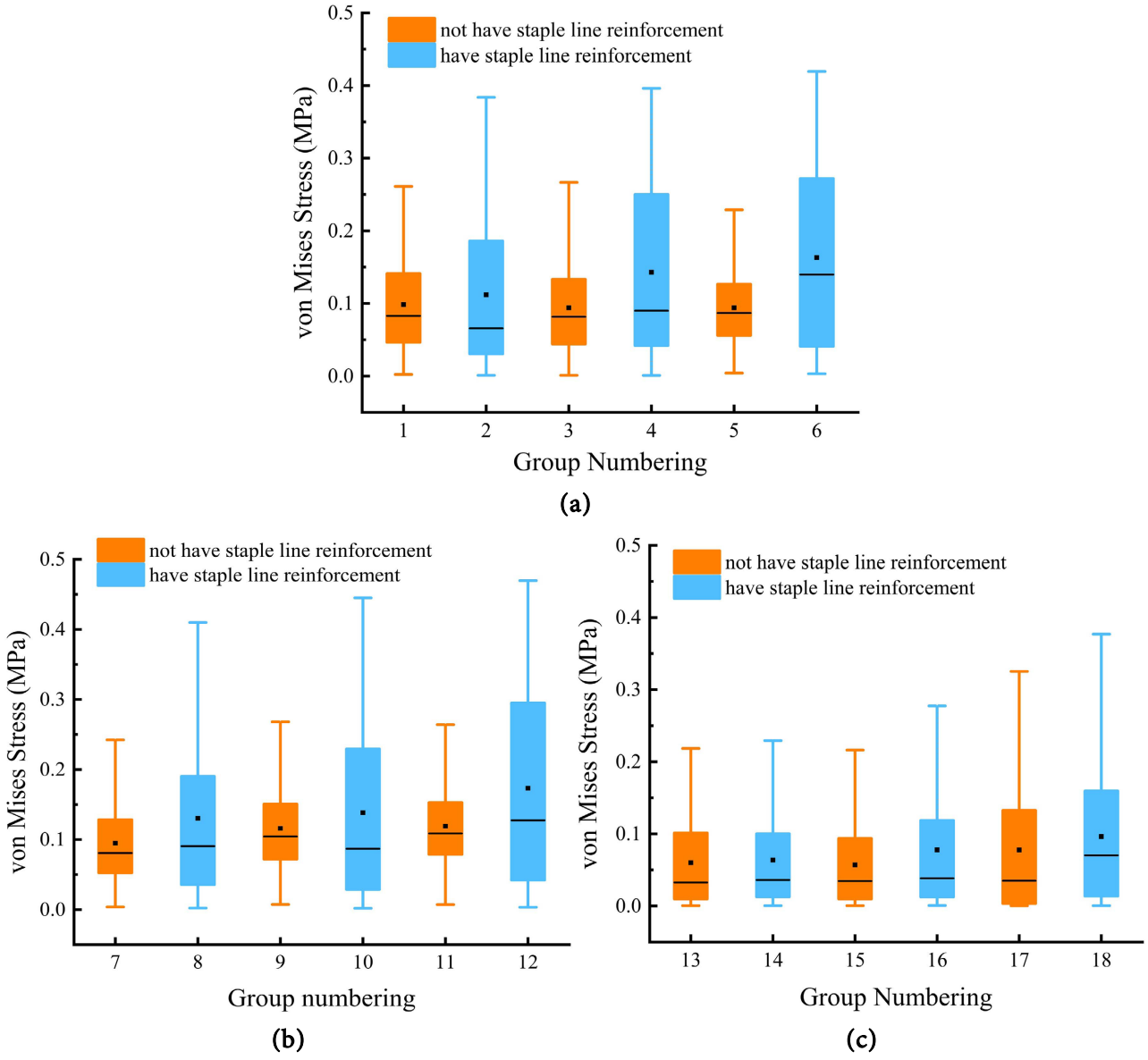

Figure 6. Tissue anastomosis stress distribution. (a) Stress distribution of stomach tissue model; (b) Stress distribution of intestine tissue mode; (c) Stress distribution of lungs tissue model.

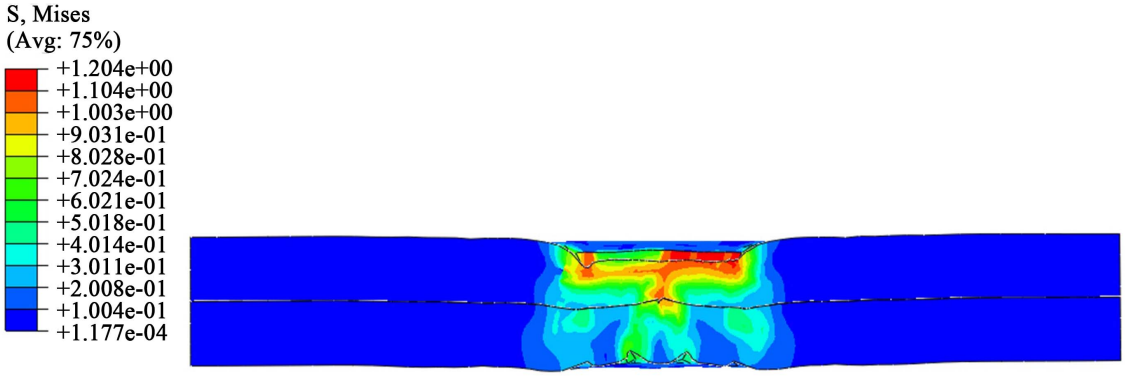

(a)

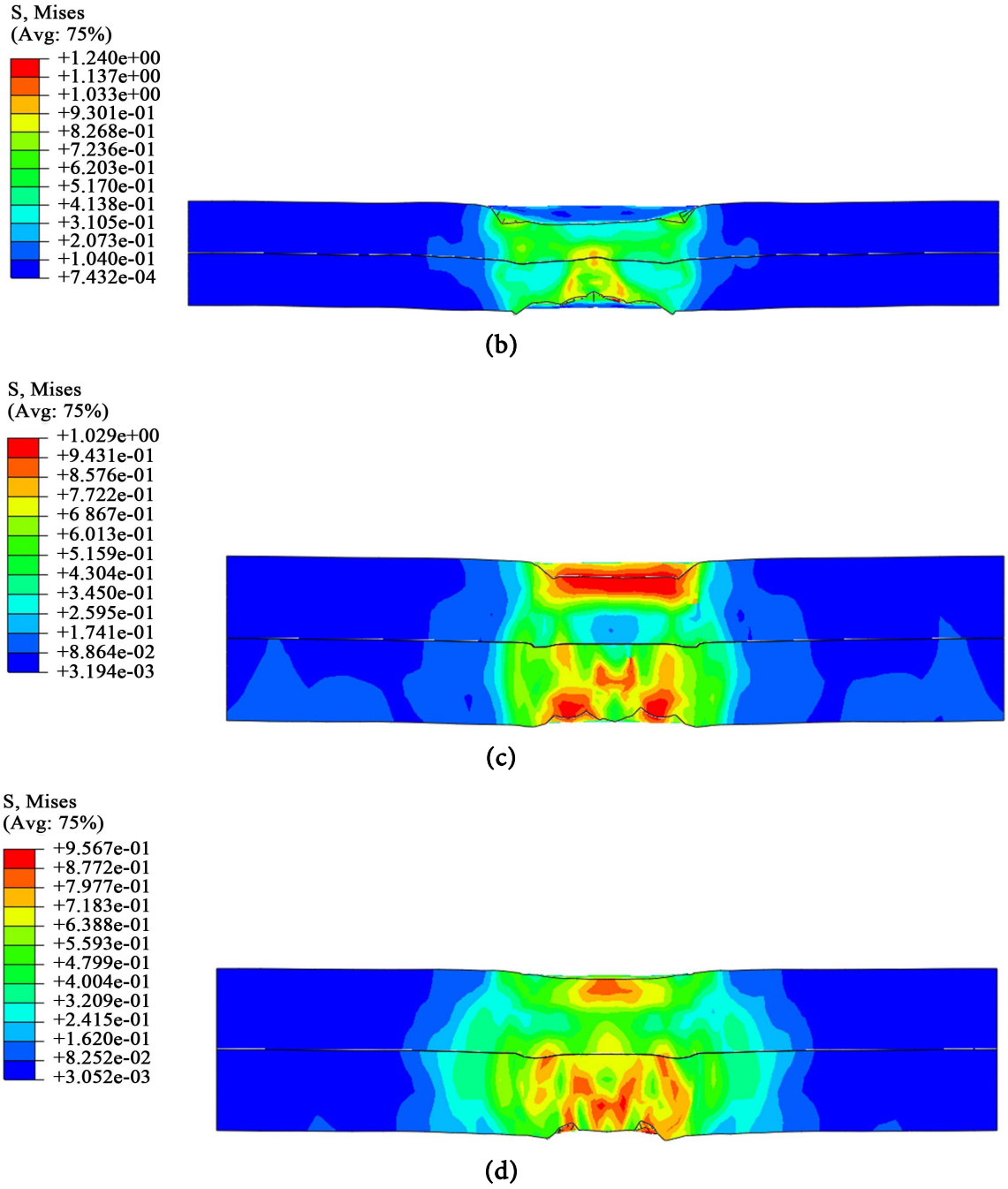

Figure 7. **(a) Force cloud of lungs tissue model without staple line reinforcement under blue staple; (b) Force cloud of lungs tissue model with staple line reinforcement under blue staple; (c) Force cloud of the stomach tissue model without staple line reinforcement under green staple; (d) Force cloud of the stomach tissue model with staple line reinforcement under green staple.**

Figure 7(d) shows that with the use of the reinforcement, it can be seen that the areas of high stress in the tissue are dispersed to the periphery and are more evenly distributed.

4.2. Evaluation of Leak-Proof Performance of the Staple Line

The results of the leak-proof performance test of the staple line are shown in Table 3.

Table 3. Results of sealing performance testing for staple line.

Tissue type	Group numbering	Pressure values (kPa)	
		Control group	Experimental group
Stomach	1	9.3	12.1
	2	7.8	8.1
	3	10.1	11.2
	4	8.6	10.5
	5	7.9	11.3
	Standard deviation	0.87	1.37
Intestine	1	7.1	9.7
	2	9.8	9.1
	3	7.0	12.7
	4	8.2	10.9
	5	9.3	11.6
	Standard deviation	1.13	1.29
Lungs	1	3.9	4.5
	2	4.1	5.3
	3	3.2	4.9
	4	3.4	6.1
	5	4.1	4.7
	Standard deviation	0.37	0.57

When the air pump continued to apply pressure, intestinal leakage test experimental group 5 appeared to burst the intestinal body during the experiment, and the section with the staple line reinforcement was used with good results and did not produce air leakage. The pressure values of the tissue leakage were calculated as follows: the average pressure value of the gastric incision margin in the control group was 8.74 kPa, and the average pressure value of the gastric incision margin in the experimental group was 10.64 kPa; the average pressure value of the intestinal section in the control group was 8.28 kPa, and the average pressure value of the intestinal section in the experimental group was 10.8 kPa; the average pressure value of the pulmonary incision margin in the control group was 3.74 kPa, and the average pressure value of the lung section in the experimental group was 5.1 kPa; and the average pressure value of the pulmonary incision margin in the control group was 5.1 kPa. The average pressure value of the control group was 3.74 kPa, and the average pressure value of the experimental group was 5.1 kPa. In the combined leak-proof performance experiments of the three different tissues, the anastomosis with the staple line reinforcement was subjected to a higher-pressure value than that of the direct anastomosis with the anastomosis, and this pressure value difference was more than 20%, which can be analyzed to conclude that the reinforcement line has a good tissue reinforcement effect on the anastomosis.

5. DISCUSSION

With the increasing frequency of use of surgical anastomoses, each model of anastomosis is given a range of surgical types and tissue thicknesses that are compatible with each other, but due to individual and tissue differences, damage to the portion of the staple in contact with the tissue occurs when the anastomotic tissue pressure is greater than the safe pressure value. Excessive anastomotic pressure causes local

tissue apoptosis and triggers inflammation, which leads to a delayed repair period and affects collagen deposition and tissue healing. Physicians can only rely on the product instructions provided by the manufacturer of the stapler, training, and extensive experience in clinical trials to select the appropriate staple cartridge during use.

For stomach tissues, an anastomotic pressure value of 78.4 kPa is required for effective tissue closure, while for intestinal tissues an anastomotic pressure value of 58.8 kPa is required [17]. The model in this paper without the use of the staple line reinforcement showed that the trend of concentration of the stress values had some parts that did not reach the required anastomotic pressure values, while areas of high stress could be seen in the cloud diagrams in the part where the staple was pressed. It has been shown that the pressure of the anastomotic staple on the soft tissues exceeding 220 kPa may cause inflammation of the tissues [26], while the anastomotic staple forming height, anastomotic staple forming condition, tissue thickness, and tissue compression characteristics all contribute to the stress abnormality on the anastomotic surface of the tissues. In the field of mechanical properties of anastomotic staples on soft tissues, Novácek proposed the design of multiple rows of anastomotic staples with variable heights [27], thus allowing the tissues to achieve the desired uniform stress. Subsequent research on the use of staple line reinforcement sheets could incorporate a multiple-row anastomotic staple model design, and analyses the variation of the stress between the staple and the staple, so that the mechanical properties presented in the model would be more closely aligned with the clinical scenarios in which they are used.

6. CONCLUSION

The use of BM and SIS composite extracellular matrix staple line reinforcement reduces the stress concentration of the staple around the anastomosis by increasing the contact area of the anastomosis and dispersing the forces. This material is effective in filling the void around the staple, providing additional support and stability, thus improving the mechanical properties of the anastomosis, and the use of staple line reinforcement improves the safety of surgical procedures.

CONFLICTS OF INTEREST

The authors declare no conflicts of interest regarding the publication of this paper.

REFERENCES

1. Reddy, B.N., Subhash, M., Vangel, M., Markowiak, S., Delvadia, D., Razdan, S., *et al.* (2023) Mortality Related to the Use of Stapler Devices and Clip Appliers: Analysis of the Food and Drug Administration Manufacturer and User Facility Device Experience Database. *Surgery*, **173**, 1184-1190. https://doi.org/10.1016/j.surg.2022.11.013
2. Betzold, R. and Laryea, J.A. (2014) Staple Line/Anastomotic Reinforcement and Other Adjuncts: Do They Make a Difference? *Clinics in Colon and Rectal Surgery*, **27**, 156-161. https://doi.org/10.1055/s-0034-1394089
3. Ghosh, S., More, N. and Kapusetti, G. (2022) Surgical Staples: Current State-of-the-Art and Future Prospective. *Medicine in Novel Technology and Devices*, **16**, Article ID: 100166. https://doi.org/10.1016/j.medntd.2022.100166
4. Myers, S.R., Rothermel, W.S. and Shaffer, L. (2011) The Effect of Tissue Compression on Circular Stapler Line Failure. *Surgical Endoscopy and Other Interventional Techniques*, **25**, 3043-3049. https://doi.org/10.1007/s00464-011-1667-4
5. Amani, H., Habibey, R., Hajmiresmail, S., Latifi, S., Pazoki-Toroudi, H. and Akhavan, O. (2017) Antioxidant Nanomaterials in Advanced Diagnoses and Treatments of Ischemia Reperfusion Injuries. *Journal of Materials Chemistry B*, **5**, 9452-9476. https://doi.org/10.1039/C7TB01689A
6. Shikora, S.A. and Mahoney, C.B. (2015) Clinical Benefit of Gastric Staple Line Reinforcement (SLR) in Gastrointestinal Surgery: A Meta-Analysis. *Obesity Surgery*, **25**, 1133-1141.

https://doi.org/10.1007/s11695-015-1703-x

7. Lin, X.X., Wang, W.B., Zhang, W.J., Zhang, Z.Y., Zhou, G.D., Cao, Y.L., *et al*. (2017) Hyaluronic Acid Coating Enhances Biocompatibility of Nonwoven PGA Scaffold and Cartilage Formation. *Tissue Engineering Part C-Methods*, **23**, 86-97. https://doi.org/10.1089/ten.tec.2016.0373
8. Wood, A.J., Cozad, M.J., Grant, D.A., Ostdiek, A.M., Bachman, S.L. and Grant, S.A. (2013) Materials Characterization and Histological Analysis of Explanted Polypropylene, PTFE, and PET Hernia Meshes from an Individual Patient. *Journal of Materials Science-Materials in Medicine*, **24**, 1113-1122. https://doi.org/10.1007/s10856-013-4872-y
9. Angrisani, L., Lorenzo, M., Borrelli, V., Ciannella, M., Bassi, U.A. and Scarano, P. (2004) The Use of Bovine Pericardial Strips on Linear Stapler to Reduce Extraluminal Bleeding during Laparoscopic Gastric Bypass: Prospective Randomized Clinical Trial. *Obesity Surgery*, **14**, 1198-1202. https://doi.org/10.1381/0960892042387075
10. Downey, D.M., Harre, J.G. and Dolan, J.R. (2005) Increased Burst Pressure in Gastrointestinal Staple-Lines Using Reinforcement with a Bioprosthetic Material. *Obesity Surgery*, **15**, 1379-1383. https://doi.org/10.1381/096089205774859254
11. Badylak, S., Kokini, K., Tullius, B., Simmons-Byrd, A. and Morff, R. (2002) Morphologic Study of Small Intestinal Submucosa as a Body Wall Repair Device. *Journal of Surgical Research*, **103**, 190-202. https://doi.org/10.1006/jsre.2001.6349
12. Wong, J.B., Henninger, D.D., Clymer, J.W., Ricketts, C.D. and Fryrear II, R.S. (2020) A Novel, Easy-to-Use Staple Line Reinforcement for Surgical Staplers. *Medical Devices-Evidence and Research*, **13**, 23-29. https://doi.org/10.2147/MDER.S234156
13. Cheng, W.Y., Yang, X.X., Chen, S.S., Zhao, M.B., Zhang, J.P., *et al*. (2021) Comparative Study on the *in Vivo* and *in Vitro* Degradation Process of Biological Grafts Derived from Different Tissues. *Chinese Journal of Hernia and Abdominal Wall Surgery* (*Electronic Edition*), **15**, 97-101.
14. Cheng, W.Y., Chen, J.S., Liu, Y.T., Zhao, M.B., Wang, Q., *et al*. (2019) Experimental Assessment of Tissue Repair of Basement Membrane in Partial Thickness Defect in Abdominal Wall of Rats. *Chinese Journal of Hernia and Abdominal Wall Surgery* (*Electronic Edition*), **13**, 198-203.
15. Baker, R.S., Foote, J., Kemmeter, P., Brady, R., Vroegop, T. and Serveld, M. (2004) The Science of Stapling and Leaks. *Obesity Surgery*, **14**, 1290-1298. https://doi.org/10.1381/0960892042583888
16. Simone, C. and Okamura, A.M. (2002) Modeling of Needle Insertion Forces for Robot-Assisted Percutaneous Therapy. 19*th IEEE International Conference on Robotics and Automation* (*ICRA*), Washington DC, 11-15 May 2002, 2085-2091.
17. Egorov, V.I., Schastlivtsev, I.V., Prut, E.V., Baranov, A.O. and Turusov, R.A. (2002) Mechanical Properties of the Human Gastrointestinal Tract. *Journal of Biomechanics*, **35**, 1417-1425. https://doi.org/10.1016/S0021-9290(02)00084-2
18. Haber, H.P. and Stern, M. (2000) Intestinal Ultrasonography in Children and Young Adults: Bowel Wall Thickness Is Age Dependent. *Journal of Ultrasound in Medicine*, **19**, 315-321. https://doi.org/10.7863/jum.2000.19.5.315
19. Rawlins, L., Rawlins, M.P. and Teel II, D. (2014) Human Tissue Thickness Measurements from Excised Sleeve Gastrectomy Specimens. *Surgical Endoscopy and Other Interventional Techniques*, **28**, 811-814. https://doi.org/10.1007/s00464-013-3264-1
20. Wang, S.X., Wang, J.C. and Li, J.M. (2015) Modelling and Quality Control of Robot-Assisted Gastrointestinal Assembly. *Cirp Annals-Manufacturing Technology*, **64**, 21-24. https://doi.org/10.1016/j.cirp.2015.04.050
21. Trân, T., Novacek, V., Tolba, R., Klinge, U., Turquier, F. and Staat, M. (2011) Experimental and Computational Approach to Study Stapled Colorectal Anastomosis. *Proceedings of the International Society of Biomechanics*,

Brussels, 3-7 July 2011.

22. Gao, F., Liao, D.H., Zhao, J.B., Drewes, A.M. and Gregersen, H. (2008) Numerical Analysis of Pouch Filling and Emptying after Laparoscopic Gastric Banding Surgery. *Obesity Surgery*, **18**, 243-250. https://doi.org/10.1007/s11695-007-9314-9
23. Hampton, C.E. and Kleinberger, M. (2018) Material Models for the Human Torso Finite Element Model. US Army Research Laboratory (ARL), Aberdeen Proving Ground.
24. Naini, A.S., Patel, R.V. and Samani, A. (2011) Measurement of Lung Hyperelastic Properties Using Inverse Finite Element Approach. *IEEE Transactions on Biomedical Engineering*, **58**, 2852-2859. https://doi.org/10.1109/TBME.2011.2160637
25. Saraf, H., Ramesh, K.T., Lennon, A.M., Merkle, A.C. and Roberts, J.C. (2007) Mechanical Properties of Soft Human Tissues under Dynamic Loading. *Journal of Biomechanics*, **40**, 1960-1967. https://doi.org/10.1016/j.jbiomech.2006.09.021
26. De, S., Rosen, J., Dagan, A., Hannaford, B., Swanson, P. and Sinanan, M. (2007) Assessment of Tissue Damage Due to Mechanical Stresses. *International Journal of Robotics Research*, **26**, 1159-1171. https://doi.org/10.1177/0278364907082847
27. NovÁCek, V., Trân, T.N., Klinge, U., Tolba, R.H., Staat, M., Bronson, D.G., *et al.* (2012) Finite Element Modelling of Stapled Colorectal End-to-End Anastomosis: Advantages of Variable Height Stapler Design. *Journal of Biomechanics*, **45**, 2693-2697. https://doi.org/10.1016/j.jbiomech.2012.07.021